



ELSEVIER

Agricultural and Forest Meteorology 72 (1995) 243–260

AGRICULTURAL  
AND  
FOREST  
METEOROLOGY

## Assessment of local agroclimatological conditions—a methodology

Mats Söderström\*, Bo Magnusson

*Department of Physical Geography, University of Göteborg, Reutersgatan 2 C, S-413 20 Göteborg, Sweden*

Received 4 October 1993; revision accepted 5 April 1994

---

### Abstract

A method for the assessment of climatological conditions of importance for agricultural planning and management is presented as a case study in an 80 km<sup>2</sup> area in southwestern Sweden. The method is based on the use of a geographical information system, GIS. Digital elevation data of high quality are now available in Sweden, and can be used for estimations of potential solar radiation for slopes with different inclinations and aspects. Other variables needed are digital maps of land use and mobile surveys of temperature.

The effect on potential crop growth of the radiation differences is assessed with a so called radiation index, RI. Because of the flatness of the case study area, the impact of radiation differences is generally fairly small, but it is possible with this method to locate the most and least favourable pieces of ground.

Temperatures were measured on five recording surveys. The spatial distribution of temperature on agricultural land is analyzed by a geostatistical interpolation method based on kriging. As temperature differences vary spatially in a consistent way during clear, calm nights, geostatistical modelling of measured temperatures combined with an analysis of land use should be appropriate for depicting agricultural areas which are relatively colder or warmer than average. The experimental variograms are all spherical and the ranges are from 1400 m to 4000 m. On some occasions, an anisotropy following the wind direction is detected. A relative temperature variation index, RTVI, is calculated for the kriged temperatures. As expected, the areas of cold air are located in the valley bottom and follow the contour lines fairly well, while relatively warm areas are found exclusively on hills.

The cold air drainage pattern is modelled using the GIS network analysis function. On the basis of digital elevation data, the surface can be treated as a mosaic of planes on which two forms of flow occur—channel and overland. Flow takes place over each polygon and into the neighbouring one in the direction of steepest slope.

---

\*Corresponding author.

As the results in all parts are stored in digital form, the GIS can be used to produce a general agroclimatological map for the area. The advantage of computerized map and data storage is its flexibility. It is possible to combine and display data according to requirement.

---

## 1. Introduction

Topography exerts a major influence on local climate. For agricultural purposes, a knowledge of the local differences in climate within a relatively small area is important. The growing period in northern latitudes is the greatest limiting factor to crop productivity, and small shifts in temperature have a great effect on the length of the growing season. Hence, in these regions, there is a great need for maps showing the occurrence and distribution of low temperatures over cultivated land. A minimum air temperature of 5 or 6°C is often assumed for growth of temperate crops and about 10°C for crops such as maize.

The major mode of energy exchange between plants and the environment is radiation. It provides the main energy input to plants, and this energy is converted into heat and activates other processes. There are four main ways in which radiation is important for plant life: thermal effect, photosynthesis, photomorphogenesis and mutagenesis (Jones, 1992). For cloudless conditions, the daily total direct beam solar radiation can be calculated for any slope with any aspect. The agricultural importance of differences in radiation input have been described by several authors. According to investigations by Rorison and Sutton (1975) in central England, there was a rise in maximum soil temperature on a north slope of 1°C for every 3 MJ m<sup>-2</sup> day<sup>-1</sup> of global radiation and, on a south slope, a 1°C rise for every 1 MJ m<sup>-2</sup> day<sup>-1</sup>. Rouse and Wilson (1969) showed that soils on north slopes (on a site near Montreal, Canada) had retained 50% more water than their southern counterparts by early spring, and that both air and soil temperatures are always higher on south than on north slopes, the differences being greatest in leaf-bare, snow-free periods. The potential solar radiation can be estimated by different methods. Gloyne (1965) presented an application of a simple graphical technique. Garnier and Ohmura (1968) placed a grid over a topographic map, determining the slope angle and aspect for each grid.

Climatological mapping techniques have been discussed in several reports, e.g. in Knoch (1963); Gol'tsberg (1969); Sly and Coligado (1974); Hess et al. (1975); Williams et al. (1980); Mattsson and Nordbeck (1981); Lindqvist and Mattsson (1989); Lomas et al. (1989) and Kalma et al. (1992). The maps are intended to distinguish local areas with topoclimates which differ obviously from the normal topoclimate in the area. The Swedish Council for Planning and Coordination of Research, FRN (1986) concluded that the development and adaptation of methodologies in agroclimatological mapping suitable to Swedish conditions is a matter of great concern. However, few practical examples have been presented since then. Recent developments in computer-based cartography offer new possibilities for topoclimatological surveying. In extensive agroclimatological studies, measurements

of all parameters in all places in question are practically impossible. The purpose of this paper is to describe a rapid method for spatial assessment of basic agro-climatological conditions on the local scale. Such an analysis should facilitate general planning of crop production, or can simply be used as a tool for identifying areas for which complementary field measurements are of additional importance.

## 2. The case study area

The case study area covers about 80 km<sup>2</sup> and is located in the parish of Götene, Skaraborg county, in southwestern Sweden (Fig. 1). Most of the area consists of open and undulating terrain with small forested areas. The area borders to the north on Kinnekulle, which is a table mountain composed of sedimentary rocks and dolerite.

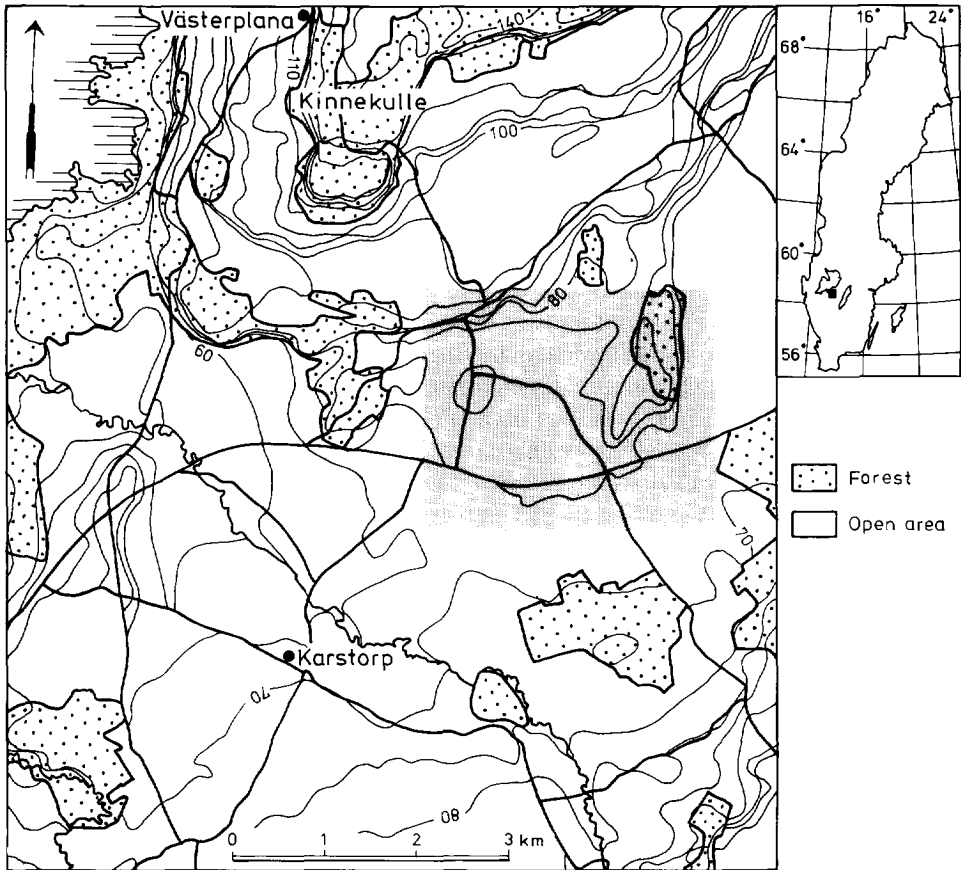


Fig. 1. The case study area in southwestern Sweden bounded by Lake Vänern. The reference weather recording station is located at Karstorp and Västerplana is a synoptic weather recording station. The shaded area indicates the location of the area mapped in Fig. 7.

In the northwest, the area is bounded by Lake Vänern, one of Europe's largest lakes (5500 km<sup>2</sup>). Elevations vary between 44 and 160 m above sea level. The summit of Kinnekulle reaches 306 m. Clay soils dominate in the central part and till in the northern part. Elsewhere, there are soils with a high percentage of sand. In addition to winter wheat, oats, oilplants and grassland agriculture, there is large scale vegetable cultivation and gardening. There is, for example, considerable cultivation of black currants, which are particularly sensitive to spring frosts during flowering.

At the synoptic weather station at Västerplana, in the northern part of the case study area, the annual average temperature was +6.0°C and the precipitation 618 mm during the most recent standard period (1961–1990). The average length of the growing season for the region is 200 days and the daily minimum temperature during the period 1980–1990 (May–September) at screen level was below 0°C on 13 occasions at Västerplana. During three seasons (1988–1990), from 1 April to 30 September, there were 37 occasions of cloudless, calm nights. This occurred most frequently in May, when plants are particularly sensitive to low temperatures.

### 3. Methods and materials

Geographical information systems (GIS) are sets of computer tools for collecting, storing, retrieving, transforming and displaying spatial data from the real world (Burrough, 1986). The data used are separated into three types: points, lines and areas. Each entity is labelled so that non-spatial descriptive information in a database management system can be accessed in geographical analyses. These analyses might, for example, be combinations of different maps for the production of a new map which responds to a specific demand. Other examples are reclassification of maps or simplification through merging of neighbouring map units. In this study, PC Arc/Info 3.4D plus (ESRI, 1992) was run on a 486/33 computer.

Three-dimensional modelling is also possible in many GIS. SEM version 1.2.2 (ESRI, 1991) is a so-called structured elevation modelling module for PC Arc/Info 3.4. The program uses the technique of triangulation, which is designed for irregularly spaced data points. A three-dimensional surface, represented by non-overlapping triangles based on Delaunay triangulation, is constructed by lines connecting points that have  $x$ -,  $y$ -, and  $z$ -values. This makes up a so-called triangulated irregular network (TIN). The TIN model has vector topology, and information on each surface, such as area, aspect, slope and  $z$ -value, is stored in an attribute database.

A variety of digital data are available from the Land Survey of Sweden (Ottosson and Rystedt, 1991). Digital elevation data on a 50 m regular grid constitute the basis for this study. Data are stored in three columns: two geographical coordinates and the elevation at the location defined by the coordinates. A point spacing of 200 m was considered sufficient for the aim and scale of this study. The size of the 4000 triangular polygons created from this database is 2 ha, each of which receives a unique value of aspect and slope. Here, the descriptive attributes are stored in dBASE format. The set of equations A1–A10 (Appendix) were written as a macro program in dBASE for the estimation of direct incoming solar radiation ( $R_i$ ) on each open-land, 2 ha TIN

polygon. The hourly measurements of global radiation at the reference station during cloudless conditions are used as ‘true’ values for horizontal ground for the whole area.

The importance of the radiation differences for cultivation can be estimated with a so-called radiation index, RI. The results for 25 April 1993, which was a cloud-free day, is used here as an example. The RI is part of a growth index which is included in a crop growth model developed by Torssell et al. (1982). RI is calculated from

$$RI = [1 - e^{(-kR_i/R_{\max})}](1 - e^{-k})^{-1} \quad (1)$$

where  $R_{\max}$  is insolation at photosynthetic saturation of the stand, and  $k$  is a constant determining the curvature of the radiation response curve. RI is a number between 1 (optimal radiation conditions) and 0. The actual effect on crop growth is a combination of several parameters in the model. For a crop with a leaf area index of 5–10, they found that  $R_{\max} = 29.31 \text{ MJ m}^{-2} \text{ day}^{-1}$  and  $k = 2$ .

For the analysis of cold air drainage, a lack of computer power forced us to further decrease the number of digital elevation data points used. An elevation contour map was produced from the regularly spaced (200 m grid) elevation data. The isolines were converted to irregularly spaced elevation data points, which was used to create a TIN model consisting of 1600 polygons. Such an operation does not automatically lead to the loss of information, as a TIN allows extra data points in areas of complex relief, while data in relatively homogenous terrain can be fairly sparse.

Information on land use was derived from official topographical map sheets (scale 1:50 000). The investigation area is fairly homogeneous, in general consisting of forested areas, pasture or cultivated land. This information, together with roads and hydrography, was digitized as separate maps.

Temperature measurements were carried out through mobile surveys, which have been used in many studies to describe topoclimate. Lomas et al. (1969) used mobile measurements to map frost areas in Israel. The results showed a close relationship between low temperature and topography variations. The equipment in the present study consists of a micrologger (Campbell Scientific Inc., Logan, UT, Model 21X) and three thermocouples of type T (copper constantan). The latter were calibrated ( $\pm 0.15^\circ\text{C}$ ) in a climatic chamber before and after the investigations. A thermistor inside the logger was used for calculation of the reference temperatures. Air temperatures were recorded at 0.3, 1.0 and 2.0 m above the road surface. Only data from the 2.0 m level were used for mapping. Data were recorded every 10 s at a speed of about  $50 \text{ km h}^{-1}$ . The prevailing weather conditions during a measuring trip are very important. The road stretch was mapped over a 1 h period and the measurements were started just after sunset in clear ( $\leq 2$  octas) and calm ( $\leq 2 \text{ m s}^{-1}$  at 10 m above ground) weather on five occasions during 1989–1993. To compensate for the general temperature decrease during the measuring trip, temperature recordings were made continuously at the reference station as well as twice (with a time lapse) at a few other locations. The reference station in the central part of the study area (Fig. 1) hourly records temperature and humidity (Rotronic, Zurich), solar radiation (LI-COR Pyranometer, LI-COR Inc., Lincoln, NB), heat flux (Heat Flow Transducer), wind and wind direction (Young Wind Monitor, R.M. Young Co., Traverse City, MI) on a

Campbell Scientific Inc. CR10 datalogger. The temperature change, which was assumed to be linear, was utilized for adjustment of the observed temperatures.

A method for assessing the importance of the temperature variation for agriculture in an area was described by Houvila (1964). He developed a so-called frost risk index classification based on the deviation of the individual adjusted temperatures  $T$  from the mean value of the observations  $T_{\text{mean}}$ . The mean deviation  $e$  is defined as

$$e = n^{-1} \sum_{i=1}^n |T_i - T_{\text{mean}}| \quad (2)$$

where  $n$  is the number of observations. If the frequency distribution is normal, the mean deviation will be independent of the range of the observed temperature values. An index value of 1, areas with the highest temperature, is given to observation points at which the temperature  $T$  deviates by more than  $3e$ ; index 2 if  $2e$  is less than  $T$  and less than or equal to  $3e$ ; index 3 if  $e$  is less than  $T$  and less than or equal to  $2e$ , and so on to the highest index of 8 for points with  $T$  less than or equal to  $-3e$ . As our purpose is not to assess frost risk, but merely to point out areas which are colder or warmer, we prefer to rename this index as a relative temperature variation index, RTVI.

When the local variance of sample values is controlled by the relative spatial distribution of these samples, geostatistics can be used for spatial interpolation (Matheron, 1971). Several authors have compared different estimation techniques and reported that kriging normally gives the best result (e.g. Burrough, 1986; Isaaks and Srivastava, 1989). Kriging is essentially a weighted moving average technique in which the set of weights assigned to samples is chosen so that the estimation variance is minimized. This variance is computed as a function of the model variogram, where the variogram is calculated using the relative locations of the samples. The variogram,  $\gamma_{(h)}$ , is a function of the (lag) distance of separation

$$\gamma_{(h)}^* = (2n)^{-1} \sum_{i=1}^n [V(x_i) - V(x_{i+h})]^2 \quad (3)$$

where  $n$  is the number of pairs of samples separated by the lag distance  $n$ ,  $V(x_i)$  is the value at a point  $i$ , and  $V(x_{i+h})$  is the value at a point separated from  $i$  by a distance  $h$ .  $\gamma^*(h)$  is the experimental variogram constructed from the observations. The next step is to fit a model (Fig. 2) to the experimental data. The type and shape of the variogram determines the weights  $\lambda_j$  needed for local interpolation in the kriging process. The minimum variance unbiased estimation  $Z(x)$  is then obtained with

$$Z(x) = \sum_{j=1}^n \lambda_j Z(x_j) \quad (4)$$

where the  $Z(x_j)$ s are the values of the observations. Kriging can either be performed as point estimations in specific locations or as average estimations for blocks arranged on a regular grid. A practical introduction to kriging can be found in textbooks such as Isaaks and Srivastava (1989).

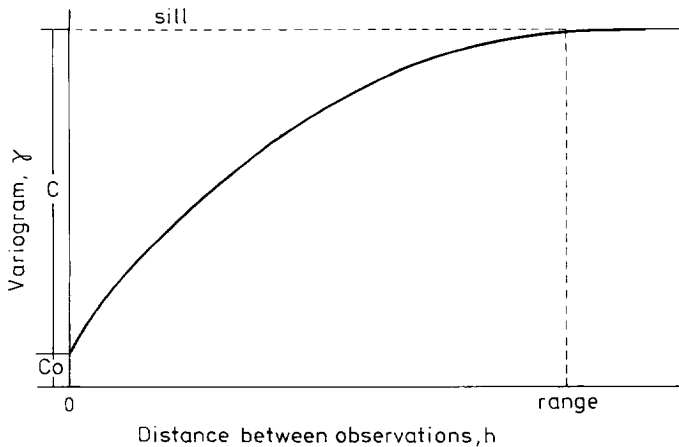


Fig. 2. Typical variogram with a spherical model. The distance at which samples become independent of each other is called the 'range',  $R$ . At this point, the variogram levels off—the 'sill',  $C + C_0$ . The latter ( $C_0$ ), known as the 'nugget variance', is an effect of measurement errors and spatial variations that occur over distances shorter than the sampling spacing.

## 4. Results and discussion

### 4.1. Potential solar radiation

This case study was carried out on a relatively flat landscape. A TIN model was produced from the 200 m grid of digital elevation data. Estimations of slope inclinations and aspects are based on this model. The inclinations are logarithmically distributed (median,  $0.8^\circ$ ; mean,  $1.2^\circ$ ; and max.,  $13.9^\circ$ ) and 62% of the area shows an incline of less than  $1^\circ$ . Most slopes with an inclination greater than  $5^\circ$  are found concentrated in bands in the northern part of the area (cf. the elevation contours on Fig. 1), and they actually coincide with the escarpments of different bedrock layers on Kinnekulle mountain. A westerly aspect ( $270^\circ \pm 22.5^\circ$ ) is most common (18%), followed by aspects towards the northwest (17%).

The average estimated radiation index, RI, is 0.88 (min., 0.83; max., 0.94), and only a small number of 2 ha fields differ by more than a few units. Hence, because of the flatness of the case study area, the impact of radiation differences on crop production is generally fairly small, but it is possible with this method to locate the most and least favourable pieces of ground. The RI differences would probably be greater if the initial digital elevation data point density had not been decreased. Not surprisingly, the sunniest sites are found on the south slopes of Kinnekulle, while shadier areas are common to the south (see Fig. 9), where northerly slope aspects are abundant. The global radiation changes with the time of year. Later during the growth period, the solar zenith angle is smaller and the slope inclination and aspect become less important, and hence the relative variation becomes even smaller.

## 4.2. Risk assessment of low temperatures

The spatial distribution of temperature variation is important for locating areas more suitable than others for growing certain crops. To spatially analyse the temperatures during the measured surveys, each temperature recording site was digitized. In this study, we were interested only in the conditions over agricultural land. During calm and clear nights, it is generally warmer within forests or groups of trees (e.g. Utaaker, 1991). The GIS was used to delete recording sites located in or very close to forests. The results from five measuring trips were treated geostatistically, and 211 observation points were found to be common to all trips. To be able to compare the multitemporal temperature recordings, the data were normalized, i.e. organized from 0 to 1 according to

$$T_{\text{norm}} = (T_{\text{O}} - T_{\text{min}})(T_{\text{max}} - T_{\text{min}})^{-1} \quad (5)$$

where  $T_{\text{norm}}$  is the normalized temperature and  $T_{\text{O}}$  is the observed temperature. The experimental variograms were all spherical and the range,  $R$ , the distance at which observations are no longer correlated with one another, varied from 1400 m to 4000 m (Table 1). A directional test (of the directions E–W, NE–SW, N–S and NW–SE) showed that, on some occasions, an anisotropy could be detected that followed the wind direction. At least for variogram ‘11/6/93’ (Table 1), it was fairly obvious that a gradual increase in wind speed (from NE) influenced the temperature distribution. Variogram ‘17/6/93’ was also anisotropic but, in this case, the anisotropy did not coincide with the recorded average wind direction at 10 m. Instead, the anisotropy seemed to follow the landscape’s topography. Ordinary block kriging was used for estimating the average normalized temperature for  $500 \times 500 \text{ m}^2$  blocks. A directional search was used (the search ellipse was divided into eight sectors) to reduce the clustering effect of the sampling procedure. It was possible from the resulting maps to distinguish some common features, although they varied slightly,

Table 1  
Variogram parameter values for five recording occasions

Start time (date–hour)	$C_0$ (°C <sup>2</sup> )	$C$ (°C <sup>2</sup> )	Max $R$ (km)	Min $R$ (km)	Max $R$ (direction)	Wind at 10 m (direction–speed (m s <sup>-1</sup> ))
12/6/89–22	0.003	0.045	2.0	2.0		WSW–0.7
25/4/90–20	0.007	0.049	2.5	1.7	NW–SE	SE–2.0
10/6/93–22	0.003	0.045	3.0	3.0		NE–0.8
11/6/93–00	0.000	0.040	4.0	1.7	NE–SW	NE–3.1
17/6/93–22	0.007	0.031	2.2	1.4	NE–SW	W–2.1

All models are spherical with the equation

$$\begin{aligned} \gamma(h) &= C_0 + C[(3h(2R)^{-1}) - (h^3(2R^3)^{-1})] & \text{for } h < R \\ \gamma(h) &= C_0 + C & \text{for } h \geq R \end{aligned}$$

where  $C_0$  is the nugget variance and  $C_0 + C$  is the sill value (Fig. 2). Max and min  $R$  (range) refer to the shape of anisotropy.



probably because of small differences in wind speed and wind direction. In general, most of the variation in normalized temperature could be explained by the relative elevation. The average temperature conditions could be mapped through a combination of several recording trips. However, to exemplify the mapping technique, we chose one of the measuring trips ('10/6/93') that seemed to be relatively representative of the general temperature variation. On this occasion, an extra 134 observation points were available, which increased the spatial accuracy of the interpolation procedure.

To assess the relative temperature variation index, RTVI, for the case study area, the same kriging technique as above was used for estimating the average temperature over agricultural land. Forested areas were excluded from the temperature mapping. The model was tested against the original observations in a cross-validation procedure. One sample data point at a time was discarded and then estimated, based on the remaining sample values using the variogram model (Fig. 3). The reliability of the estimates may be checked, as the estimation error is automatically obtained in the kriging procedure (Fig. 4). The error map can be used to delimit the extent of the map area. In areas with many roads, ordinary block kriging should produce acceptable results of interpolation. Otherwise, or if interpolation must be performed in areas of great distance from the road, the relationship between topography and temperature can be utilized in the process of cokriging. The added information enters the problem through the cross-variogram, which gives the

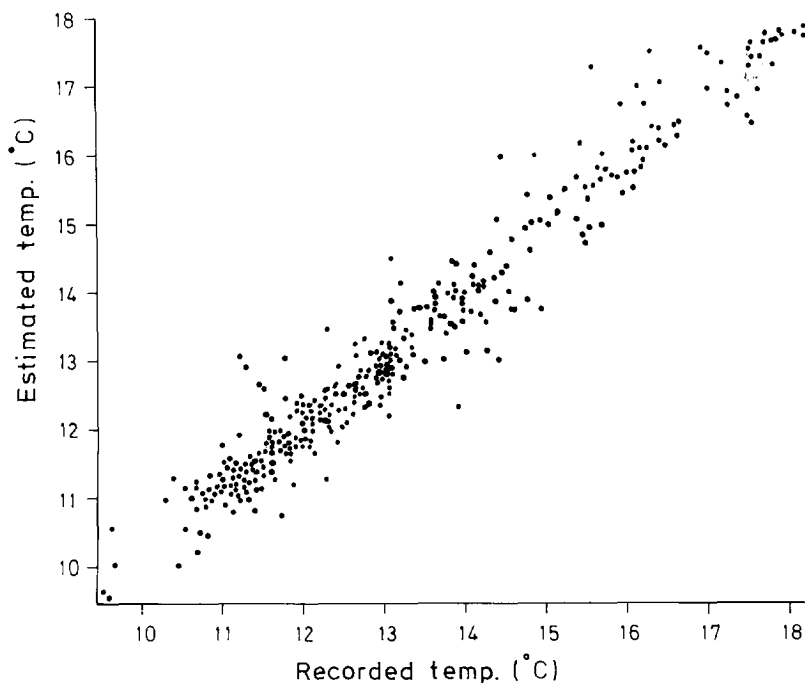


Fig. 3. Scatter plot of the kriged estimates against the recorded temperatures ( $n = 345$ ;  $r = 0.97$ ).

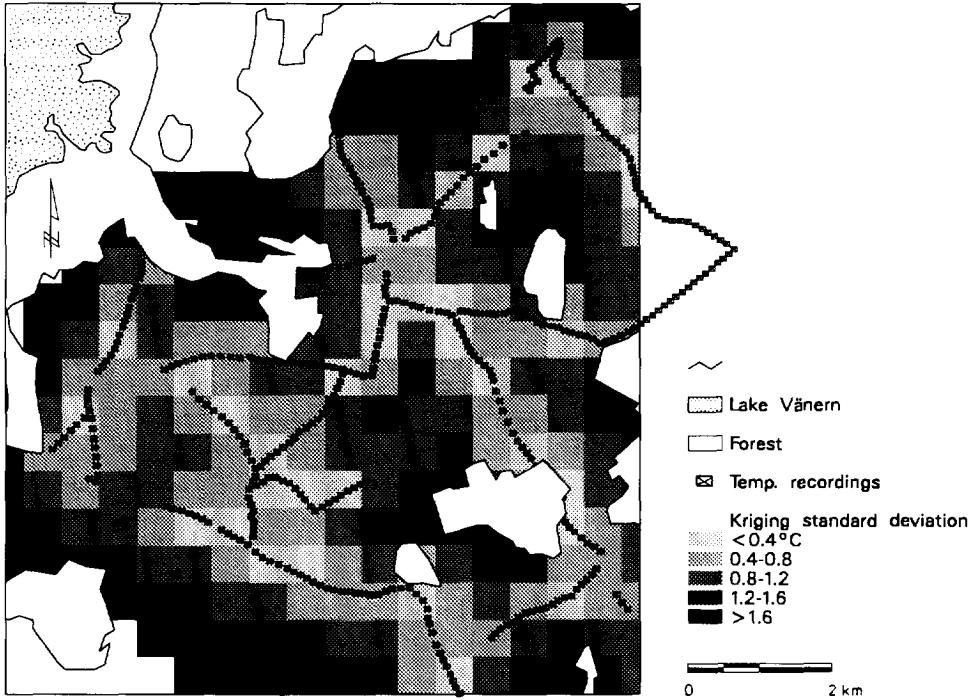


Fig. 4. Map of the estimated temperature errors (kriging standard deviation). Some temperature recording sites are located outside the actual map area, but still to some extent, they improve the estimates close to the map margin at those locations.

correlation between the two variables as a function of their separation distance (Isaaks and Srivastava, 1989). This permits the use of information on one variable to estimate the other.

A relative temperature radiation index, RTVI, was calculated for the kriged temperatures (Fig. 5). Only areas with a kriging standard deviation of less than 1.5°C (cf. Fig. 4) were mapped. As expected, the areas of cold air,  $RTVI \geq 6$ , are situated in the valley bottom and follow the contour lines fairly well (cf. Fig. 1). This is sometimes not the case, but then always in areas with less reliable estimates. The coldest area is found in the northeastern part of the map area, which is actually the lowest part of the terrain. Relatively warm areas,  $RTVI \leq 3$ , are found exclusively on hills.

#### 4.3. Cold air drainage

The cold air in the study area is probably produced to a great extent in situ. However, the mobile temperature surveys indicate the occurrence of cold air drainage (Magnusson, 1994). Fig. 6 is a plot of temperatures recorded during three

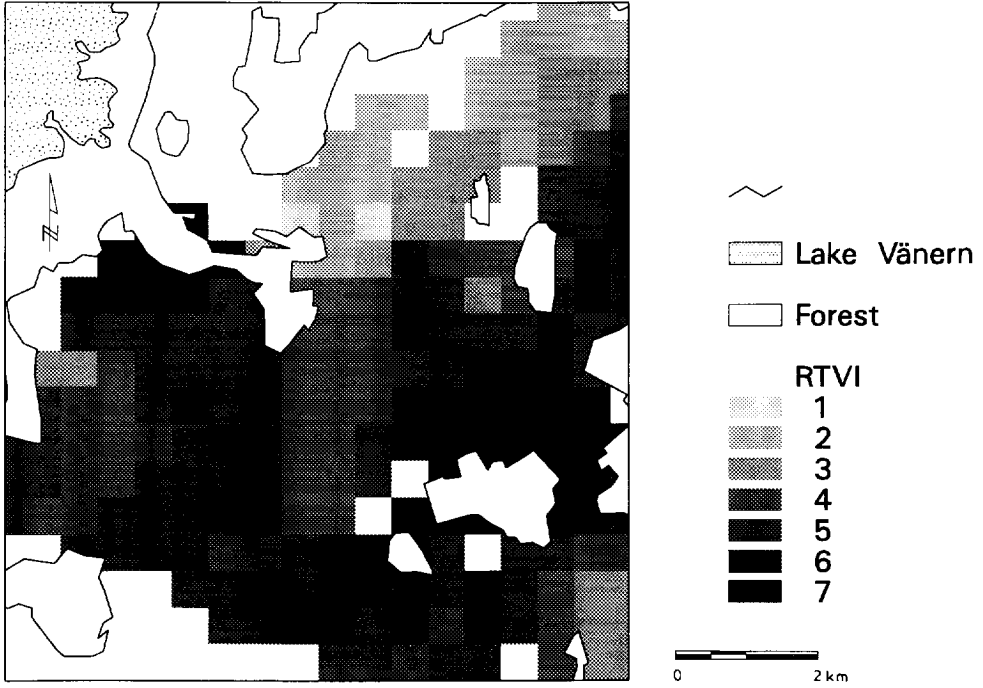


Fig. 5. Map of the estimated relative temperature variation index (RTVI). As can be expected, most of the areas of higher risk for low temperatures ( $RTVI \geq 6$ ) are found in depressions (cf. the contours in Fig. 1).

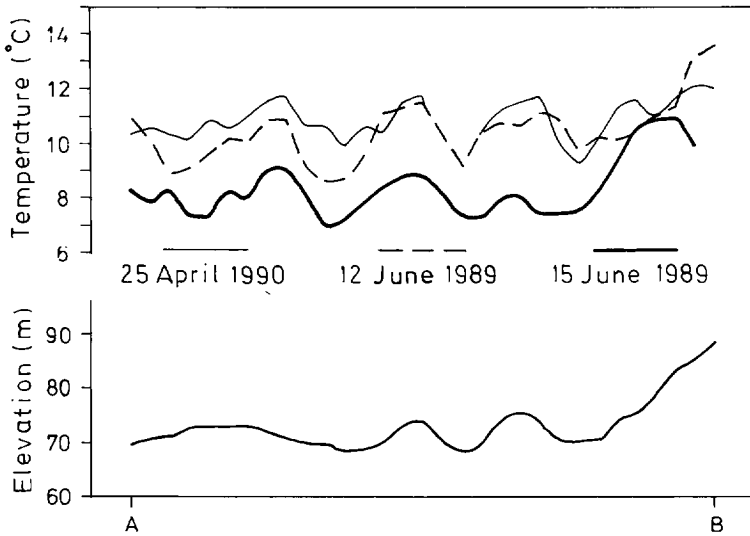


Fig. 6. The road stretch A–B in Fig. 7. Low recorded temperatures coincide very well with hollows.

mobile surveys and elevation data from the digital elevation model along the road stretch marked A–B in Fig. 7. Valleys and low temperatures correspond closely. As the transect is situated on sloping ground, this implies that cold air is probably drained towards the lower parts of the valley. On plains surrounding valleys, the cooled air layers are subject to downslope buoyancy forces, and form the basis for the drainage of cold air (Andersen and Skaar, 1987). Mattsson and Nordbeck (1981) developed a computer-based model of the formation and transportation of cold air in hilly terrain. The model was based on digitized elevation data and land use. To map the movement of cold air from the elevated areas into the cold air lakes, whose extent to a certain degree can be delimited by the geostatistical modelling, a network analysis of digital elevation data can be an appropriate and objective tool. The influence of vegetation and other obstacles is somewhat difficult to foresee. It is suggested that

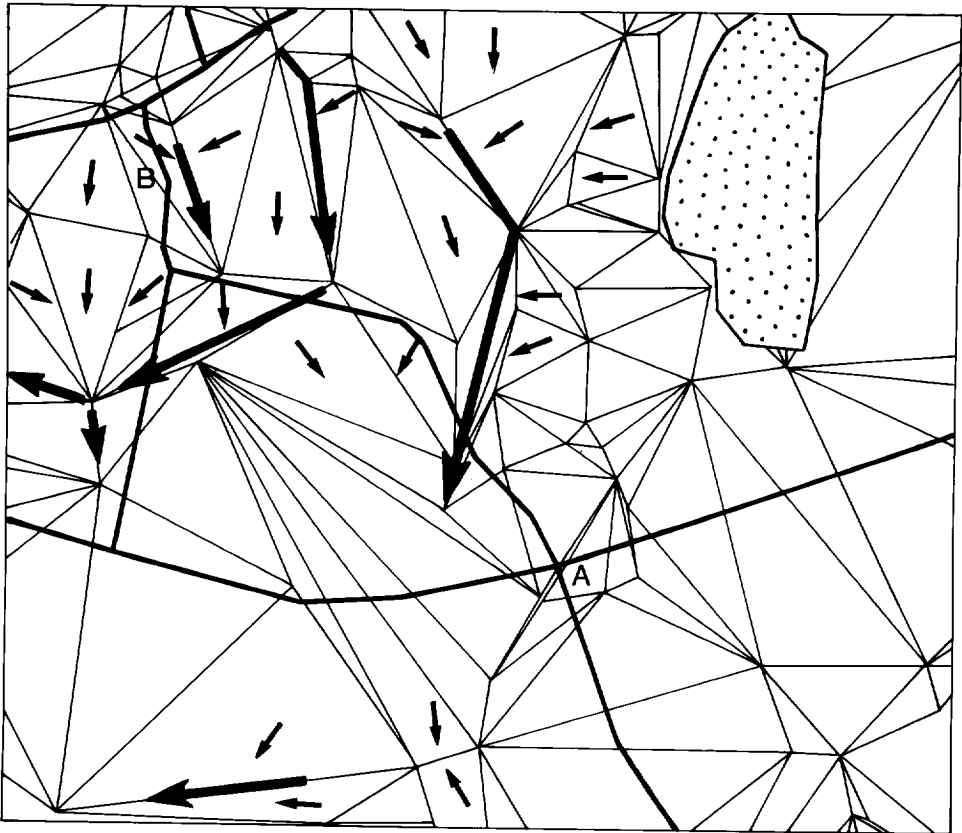


Fig. 7. Example of cold air drainage modelling with a TIN for part of the study area (see Fig. 1). The small arrows represent the slope aspect for the TIN element and the large, bold arrows indicate inclined concavities in the TIN model, where a concentrated cold air flow could occur. The road stretch A–B refers to Fig. 6. The presence of cold air drainage indicated by the TIN model is supported in Fig. 6, although it cannot be expected that the flow lines should coincide directly with the hollows in Fig. 6, as the TIN model is based on a fairly low number of data points.

mature forests might only retard the cold air flow and permit a significant subcanopy flow (Bergen, 1969; Mahrt, 1986). Other authors (e.g. Utaaker, 1979; Andersen and Skaar, 1987) mention hedges and lee plantations as sufficient for damming up the cold air flow. In the model of Mattsson and Nordbeck (1981), forested areas could not be supplied with cold air unless the cold air level in the surroundings exceeded the height of the trees. The forests in the study area are chiefly very dense plantations of Norwegian spruce. Such an obstacle could act to a great extent as a barrier. If the ground is inclined, it might direct the air flow along its edge, although in reality some throughflow would still occur. To cope with this in our TIN model, so-called break lines were incorporated around forested areas to inhibit throughflow. To find drainage networks, the surface can be treated as a mosaic of planes on which two forms of flow occur—channel and overland. Flow takes place over each triangle and into the neighbouring triangle in the direction of steepest slope (Fig. 7). Information on triangle slope direction in relation to the triangle edge makes it possible to detect concavities in the terrain where the flow is concentrated.

The cold air production is influenced by several criteria. For example, Mahrt (1986) states that: (a) the air should be slowly moving, i.e. the terrain should be relatively flat, although cold air production may also occur on slopes; (b) the heat flux from the ground should be minimal.

The latter is favoured on barren soils. According to Utaaker (1979), the most favourable areas for cold air production are mires, especially in the case of drained mires. Lindqvist and Mattson (1989) define production areas as flat or slightly inclined, open areas situated immediately on the top of a slope with cold air drainage. Such areas can easily be selected from a TIN model. In this case, we selected polygons with open land with an inclination of less than  $1^\circ$  in elevated areas close to slopes for which the flow analysis indicated the presence of air drainage (see Fig. 9).

#### *4.4. Agroclimatological mapping*

The techniques discussed in this paper can be combined for rapid assessment of agroclimatological conditions on the local scale. As the results in all parts are stored in digital form, the GIS can be used to produce a general agroclimatological map for the area. A summary of the different steps in the analysis is shown in Fig. 8. To be able to compare maps produced in other areas, it is important that the technique used is relatively objective, and possible to apply in a variety of situations. The usefulness of digital elevation data in this context certainly exceeds that of ordinary paper map contours.

Fig. 9 is an example of an agroclimatological map of the study area. However, temperature mapping has not been performed in the whole area (Fig. 5). Climatological features of interest which are possible to map with this relatively fast and simple technique include areas of high or low risk for low temperatures, sunny sites and shady sites, cold air drainage and cold air production areas. For Swedish conditions, perhaps the most important period to map is the beginning of the growth period, April–June. As general climatic information, ordinary statistics for the

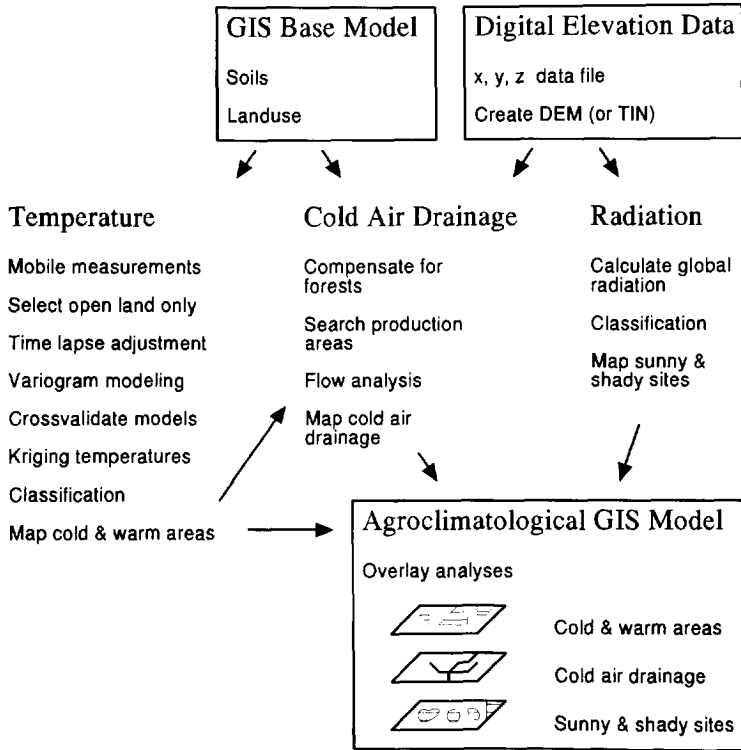


Fig. 8. Summary of the techniques used here for assessment of agroclimatological conditions.

growth period or for the whole year might be included. In this example we have used average (1961–1990) temperature, precipitation and potential evapotranspiration for the main vegetation period in the area from a nearby synoptic weather station at Skara, about 15 km southwest of the study area (Skara was used because not all information was available at Västerplana, which is the closest station). Measurements of wind direction and wind speed were not available, and thus the average wind recordings from Karstorp during 1988–1992 were used instead.

An advantage of computerized map and data storage is its great flexibility. For instance, in suitability mapping, in which the aim is to locate areas that are especially favourable for a certain type of cultivation, it is possible to combine and display data according to requirement. Digital climatological data can also be used as a data source for crop growth models (Magnusson and Söderström, 1994). Such models can quantify the impact of local climatological conditions on agriculture.

### 5. Conclusions

Agroclimatological maps are important tools for land use planning and proper management of crop production. Mapping techniques should be objective and

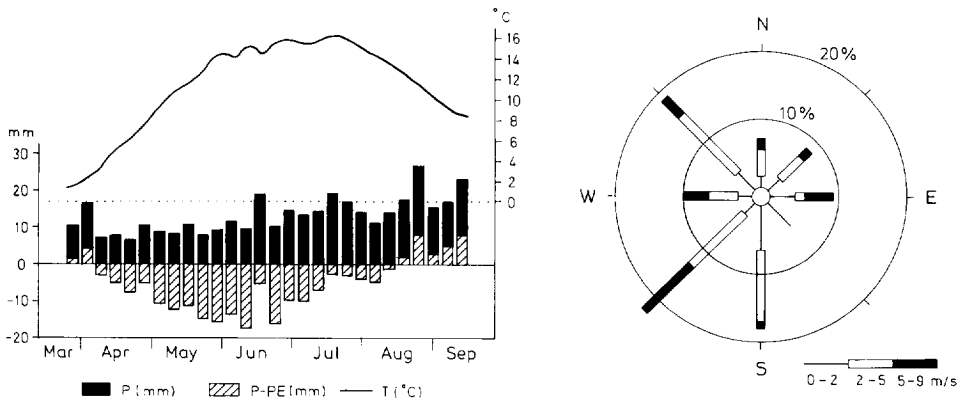
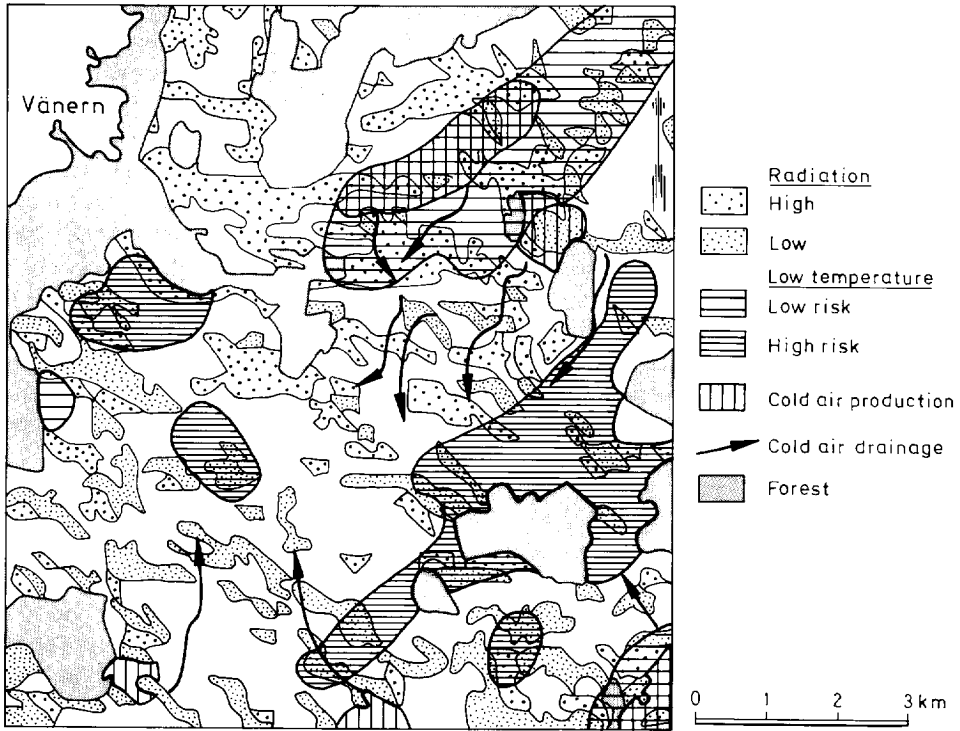


Fig. 9. An example of an agroclimatological map of the study area. Areas of high and low risk for low temperatures are defined as areas with  $RTVI \geq 6$  and  $RTVI \leq 3$ , respectively (Fig. 5). The highest and lowest 1/6 of the estimated global radiations have formed the limits for high and low radiation areas. As was shown above, the importance to crop production of these differences is fairly small. The general climatological information, weekly 30-year average (1961–1990) precipitation (P) and temperature (T), has been derived from the nearby synoptic weather station at Skara, about 15 km southwest of the study area. The potential evapotranspiration (PE) was estimated with the Penman equation. The wind rose is based on wind observations at Karstorp (Fig. 1) during 1988–1992.

possible to apply in a variety of situations. The use of GIS based digital elevation models is increasingly facilitated as digital elevation data of high accuracy become more and more accessible. Such models can be used for the rapid assessment of, e.g. potential solar radiation on the local scale. The potential effect on cultivation of the estimated radiation can be quantified with a radiation index. Temperature mapping can be carried out by mobile temperature surveys. In areas with a developed road network, cold air lakes and thermal areas might be delimited through data interpolation. Geostatistical interpolation methods based on kriging often give the best performance and, by taking into account directional effects caused, e.g. by topography or wind, it is possible to improve the estimations.

Flexibility is the most important feature of computerized map and data storage. It is possible to combine and display data according to requirement. We believe that the techniques described in this paper, a combination of mobile temperature surveys and analyses of digital elevation data, offer an adequate basis for the mapping of general agroclimatological conditions.

### Acknowledgements

The authors gratefully acknowledge the financial support provided by the foundation of Västsvenska Lantmäns Stiftelse and the technical support of Dr. S. Karlsson, Swedish University of Agricultural Sciences, Uppsala, Dr. M. S. Rosenbaum, Imperial College of Science, Technology and Medicine, London, and Professor K. Utaaker, Geophysical Institute, University of Bergen.

### Appendix

Based on the following equations, a PC Arc/Info application macro was written, mainly in dBASE, for estimation of potential solar radiation during cloud-free conditions. The program needs information on slope and aspect, which in this case is derived from the digital terrain modelling module PC SEM. The equations are mainly from Oke (1987). All angles are expressed in degrees.

(a) Declination  $\delta$

$$\delta = -23.4 \cos[360(t_j + 10)365^{-1}] \quad (\text{A1})$$

where  $t_j$  is Julian Day.

(b) Local apparent solar time  $t$

$$t = t_{\text{lst}} + (4/60 \times L) + t_{\text{eq}} \quad (\text{A2})$$

where  $t_{\text{lst}}$  is local standard time,  $L$  is longitude, and  $t_{\text{eq}}$  is the equation of time.

(c) Hour angle  $h$

$$h = 15(12 - t) \quad (\text{A3})$$

(d) Solar zenith angle  $Z$ , the angle between the sun's rays and the local zenith



direction

$$\cos Z = \sin \phi \sin \delta + \cos \phi \cos \delta \cos h \quad (\text{A4})$$

(e) Solar azimuth angle  $\Omega$ , the angle between the projections onto the horizontal plane of the sun's rays and the direction of true north measured clockwise

$$\cos \Omega = (\sin \delta \cos \phi - \cos \delta \sin \phi \cos h) / \sin Z \quad \text{for } t < 12 \quad (\text{A5})$$

$$\cos \Omega = 360 - [(\sin \delta \cos \phi - \cos \delta \sin \phi \cos h) / \sin Z] \quad \text{for } t > 12 \quad (\text{A6})$$

(f) Angle of incidence  $\Theta$ , which is the angle between the sun's rays and the normal to the slope

$$\cos \Theta = \cos i_s \cos Z + \sin i_s \sin Z (\cos \Omega \cos a_s + \sin \Omega \sin a_s) \quad (\text{A7})$$

where  $i_s$  is the slope inclination, and  $a_s$  is the slope aspect measured clockwise.

(g) According to Niels Rodskjer (unpublished data, 1981), about 20% of the incoming radiation on a clear day is still diffuse radiation. Hence, on a clear day  $S_i$ , the beam solar radiation on a plane normal to the solar beam, is related to the measured global radiation  $S_g$  according to

$$S_i = (S_g - 0.2S_g) / \cos Z \quad (\text{A8})$$

(h) The global radiation received on a slope  $S_{gs}$  can be calculated as

$$S_{gs} = S_i \cos \Theta + 0.2S_g \quad (\text{A9})$$

(i) Daily total  $S_{gs}$ ,  $S_{tot}$

$$S_{tot} = \int S_{gs} dH \quad (\text{A10})$$

where  $H$  indicates the time from sunrise to sunset.

## References

- Andersen, O.J. and Skaar, E., 1987. Production and flow of cold air in a valley topography. Part 2, Cold air accumulation in valleys, models and observation. Report 3. Geophysical Institute, Meteorological Division, Bergen, 141 pp.
- Bergen, J.D., 1969. Cold air drainage on a forested mountain slope. *J. Appl. Meteorol.*, 8: 884–895.
- Burrough, P.A., 1986. Principles of Geographical Information Systems for Land Resources Assessment. Clarendon Press, Oxford, 194 pp.
- ESRI, 1991. PC Arc/Info Structured Elevation Model (SEM) ver. 1.2.2. Environmental Systems Research Institute, Gesellschaft für Systemforschung und Umweltplanung. Ringstrasse 7, D (W)-8051 Kranzberg.
- ESRI, 1992. PC Arc/Info ver. 3.4D plus, Environmental Systems Research Institute, Inc. 380 N.Y. Street, Redlands, CA 92373.
- FRN, 1986. Svensk Agrometeorologi. Swedish Council for Planning and Coordination of Research, Report 86: 9, Stockholm, 110 pp.
- Garnier, B.J. and Ohmura, A., 1968. A method of calculating the direct short wave radiation income of slopes. *J. Appl. Meteorol.*, 7: 796–800.
- Gloyne, R.W., 1965. A method for calculating the angle of incidence of the direct beam of the sun on a plane surface of any slope and aspect. *Agric. Meteorol.*, 2: 401–410.

- Gol'tsberg, I.A. (Editor), 1969. Microclimate of the USSR. Israel Program for Scientific Translations Ltd, Jerusalem, 236 pp.
- Hess, M., Niedzwiedz, T. and Obrebska-Starkel, B., 1975. The methods of constructing climatic maps of various scales for mountainous and upland territories, exemplified by the maps prepared for Southern Poland. *Geogr. Polon.*, 31: 163–187.
- Houvila, S., 1964. On precautions against crop damage due to radiation frost within hilly regions. *Societas Scientarium Fennica, Commentationes Physico-Mathematicae XXIX*, 22 pp.
- Isaaks, E.H. and Srivastava, R.M., 1989. *Applied Geostatistics*. Oxford University Press, New York, 561 pp.
- Jones, H.G., 1992. *Plants and Microclimate*. Cambridge University Press, Cambridge, pp. 9–44.
- Kalma, J.D., Laughlin, G.P., Caprio, J.M. and Hamer, P.J.C., 1992. The bioclimatology of frost. Its occurrence, impact and protection. In: G. Stanhill (Editor), *Advances in Bioclimatology 2*. Springer, Berlin, 144 pp.
- Knoch, K., 1963. Die Landesklimaaufnahme, Wesen und Methodik. Bericht des Deutschen Wetterdienstes No. 85. Band 12.
- Lindqvist, S and Mattsson, J.O., 1989. Topoclimatic maps for different planning levels—some Swedish examples. *Build. Res. Pract.*, 5: 299–304.
- Lomas, J., Shashoua, Y. and Cohen, A., 1969. Mobile surveys in agrotopoclimatology. *Meteorol. Rundsch.*, 22: 96–101.
- Lomas, J., Gat, Z., Borsuk, Z. and Raz, Z. (Editors), 1989. Frost Atlas of Israel. Div. Agric. Meteorol., Israel Meteorol. Serv., Bet Dagan, 10 map sheets.
- Magnusson, B., 1994. Techniques for surveying agroclimatic elements—a case study in the Källby area, SW Sweden. Dept. Physical Geography, Göteborg University, GUNI Report 34, 82 pp.
- Magnusson, B. and Söderström, M., 1994. Combining crop growth models and geographical information systems for agricultural management—a case study of ley production potential as affected by local temperature variation and soil water capacity. *Acta Agric. Scand., Sect. B, Soil and Plant Sci.*, 44: 65–74.
- Mahrt, L., 1986. Nocturnal Topoclimatology. WMO Tech Note 132/WCP 117; Geneva, 76 pp.
- Matheron, G., 1971. The theory of regionalized variables and its applications. *Les Cahiers du Centre de morphologie mathématique de Fontainebleau*. Ecole Nationale Supérieure des Mines de Paris, 198 pp.
- Mattsson, J.O. and Nordbeck, S., 1981. Modelling cold air patterns. *Lund Studies in Geography, Ser. A*, No. 59, 11 pp.
- Oke, T.R., 1987. *Boundary Layer Climates*. Methuen, London, 372 pp.
- Ottoson, L. and Rystedt, B., 1991. National GIS programmes in Sweden. In: D.J. Maguire, M.F. Goodchild and D.W. Rhind (Editors) *Geographical Information Systems. Volume 2: Applications*. Longman, Essex, pp. 39–46.
- Rorison, I.H. and Sutton, F., 1975. Climate, topography and germination. In: C.G. Evans, R. Bainbridge and O. Rackham (Editors), *Light as an Ecological Factor: 2*. 16th Symposium of the British Ecological Society. Blackwell, Oxford, pp. 361–383.
- Rouse, W.R. and Wilson, R.G., 1969. Time and space variations in the radiant energy fluxes over sloping forested terrain and their influence on seasonal heat and water balances at middle latitude sites. *Geogr. Annal.*, 51A, 3: 160–175.
- Sly, W.K. and Coligado, M.C., 1974. Agroclimatic Maps for Canada—Derived Data: Moisture and Critical Temperature Near Freezing. *Tech. Bull. 81, Agric. Canada, Agrometeorol. Res. Serv., C.B.R.I., Ottawa*, 20 pp.
- Torszell, B.W.R., Kornher, A. and Svensson, A., 1982. Optimization of parameters in a yield prediction model for temporary grasslands. Swedish University of Agricultural Sciences, Department of Plant Husbandry, Report 112, 33 pp.
- Utaaker, K., 1979. Om lokale variasjoner i temperaturklimaet. *Vaeret*, 2: 50–56.
- Utaaker, K., 1991. *Mikro og lokalmeteorologi*. Alma Mater Forlag AS, Bergen, 242 pp.
- Williams, G.D.V., McKenzie, J.S. and Sheppard, M.I., 1980. Mesoscale agroclimatic resource mapping by computer, an example for the Peach River region of Canada. *Agric. Meteorol.*, 21: 93–109.